Changes in the Connections of the Main Olfactory Bulb After Mitral Cell Selective Neurodegeneration

Javier S. Recio, Eduardo Weruaga,[*] Carmela Gómez, Jorge Valero,
Jesús G. Briñón, and José R. Alonso

Department of Cell Biology and Pathology, Institute for Neuroscience of Castilla y León,
Universidad de Salamanca, Salamanca, Spain

The connections of the main olfactory bulb (OB) of the mouse were studied with iontophoretic injections of biotinylated dextran amine. To sort efferences from mitral cells and tufted cells, the Purkinje cell degeneration (*PCD*) mouse was used. This mutant animal undergoes a specific neurodegeneration of mitral cells, whereas tufted cells do not degenerate. The unilateral tracer injections used were small and confined largely to the OB of both *PCD* and control mice at P120. Seven days after tracer injection, the efferences from the OB and the centrifugal afferences from secondary olfactory structures to it were studied. Although there is a large overlap of their target fields, mitral cell axons innervated more caudal regions of the olfactory cortex than tufted cell axons, thus providing definitive evidence of the differential projections of olfactory output neurons. Additionally, an important increase in retrogradely-labeled neurons was detected in the ipsilateral anterior olfactory nucleus of the mutant animals. This was not observed in any other secondary olfactory structure, suggesting a strengthening of the centrifugal input to the OB from that central area after mitral cell loss. Moreover, we recorded a complete loss of bilaterality in the olfactory connections of the *PCD* mice due to degeneration of the anterior commissure. These results point to an important reorganization of this essential olfactory circuit between the anterior olfactory nucleus and the OB, and hint at a transsynaptic level of plasticity not considered previously in literature. © 2007 Wiley-Liss, Inc.

Key words: anterior commissure; BDA tracer; *PCD* mutant mouse; reorganization; tufted cells

The main olfactory bulb (OB) is the first processing station in the olfactory pathway. There, olfactory information is conveyed to secondary olfactory structures by output neurons, which are both mitral cells and tufted cells. Despite their morphologic similarities (Ramón y Cajal, 1911; Pinching and Powell, 1971), mitral and tufted cells do not form a homogeneous population of output neurons, because they have neurochemical, physiologic, and functional differences (Macrides et al., 1985; Nagayama et al., 2004).

Secondary olfactory structures are defined as areas of the brain to which both mitral cell and tufted cell axons project directly (Cleland and Linster, 2003). They were known formerly as "primary olfactory cortices" (De Olmos et al., 1978; Haberly, 2001). These structures can usefully be divided into three groups: the anterior olfactory nucleus (AON), the rostromedial olfactory cortex, and the lateral olfactory cortex (Shipley et al., 1996).

Hodologic olfactory studies are relatively scarce. Most of them are based on large tracer injections into the OB, which in many cases spread out of its caudal limits, entering the AON or the accessory olfactory bulb, thus hindering the study (De Olmos et al., 1978; Shipley and Adamek, 1984). Moreover, using this kind of injections it is somewhat difficult to distinguish projections from tufted and mitral cells. Haberly and Price (1977) clarified this issue partially in rats using horseradish peroxidase injections. Later, some differences were described between the projections of medial tufted cells and those of both mitral and internal tufted cells within the ipsilateral cortex (Scott et al., 1980; Scott, 1981; Schoenfeld and Macrides, 1984). However, those studies were carried out in mammals other than the mouse, which is the species of choice in many neurobiologic studies.

In our study, we carried out small injections confined completely to the OB, thus clearing up some of the pitfalls described above. Furthermore, to convincingly

discern projections from tufted and mitral cells, we used a mutant mouse that loses mitral cells whereas its tufted cells remain unaffected. This mitral cells loss is specific and postnatal, preventing developmental compensatory mechanisms. The animal used was the *PCD* (Purkinje cell degeneration) mouse (Mullen et al., 1976). The homozygous mutation results in the degeneration of Purkinje cells in the cerebellum and mitral cells in the OB, among others (Mullen et al., 1976; Fernández-González et al., 2002). The selective loss of OB mitral cells begins around 70 days after birth. Before this age, the cellular and synaptic organization in the OB seems to be normal, but along a short time window an accelerated mitral cell loss occurs, leading to an almost complete absence of these projection neurons by P90–P120. Other OB populations do not exhibit a comparable degenerative sequence (Baker and Greer, 1990), because mitral cells are the only neuronal population in the OB expressing the mutated gene. Despite mitral cell degeneration, the odor induced patterns of 2-deoxyglucose uptake in OB glomeruli are not altered (Greer and Shepherd, 1982), showing that olfactory receptor cells respond in a normal manner to odors in *PCD* mice. Moreover, TH activity and immunoreactivity remain intact in the *PCD* OB (Baker and Greer, 1990). By contrast, the tufted cells of *PCD* mice, primarily unaffected (Greer and Shepherd, 1982), constitute the only centripetal pathway to convey olfactory information to secondary olfactory structures. Thus, the *PCD* mutant mouse is a suitable model for both discerning between mitral cell and tufted cell projections in mice and for addressing phenomena of adult neural plasticity.

The main aim of this study was to carry out a hodologic study of the OB of mutant *PCD* mice, allowing analysis of the alterations induced by the *pcd^{1J}* mutation. This analysis should afford knowledge of the olfactory projections after mitral cell loss, and hence the identification of the differences in the projection patterns between mitral and tufted cells in the mouse olfactory system. Furthermore, we searched for possible compensatory mechanisms in the connections of the OB after mitral cell neurodegeneration in *PCD* mice.

MATERIAL AND METHODS

Animals

C57BL/6J mice (*Mus musculus*, L. 1758) heterozygous for the *pcd^{1J}* mutation (+/*pcd*) from a colony originally obtained from Jackson Laboratories (Bar Harbor, ME) were mated with wild-type DBA/2J females. The *pcd^{1J}* allele was associated with the genetic background of the C57BL/6J strain, whereas the normal allele was associated with the genetic background of the DBA/2J strain. Mice genotyping was carried out by PCR amplification of specific microsatellite sequences. Littermates were selected according to their genotypes for use as control (+/+) and experimental animals (*pcd*/*pcd*), or to expand the colony (+/*pcd*).

Ten *PCD* (*pcd*/*pcd*) mice and 10 control (+/+) littermate mice of 120 days of age were used in this study. The experiments were carried out in accordance with the guidelines of the European Community Council (86/609/EEC) and current Spanish legislation for the use and care of laboratory animals (RD 1201/2005).

Tracer Injections

To study the connections of the OB, 10 kDa biotinylated dextran amine (BDA; Molecular Probes Inc., Eugene, OR) was injected iontophoretically into the OB. The animals were first anaesthetized with a solution composed of ketamine (120 μg/g body weight [b.w.]), diazepam (8 μg/g b.w.) and atropine (0.48 μg/g b.w.) and were then fixed in a stereotaxic apparatus. After exposing the surface of the skull, the bone over the left OB was removed to allow open access to it. The stereotaxic coordinates for the injection in control mice were: rostral, 4.3 mm; lateral, 1.1 mm from bregma; and deep −1.1 mm from the dura. Because of the reduced brain size of *PCD* mice, the stereotaxic coordinates for the injections were first selected for control animals and thereafter transposed to the mutant mice. Thus, similar injection points were calculated in both experimental groups simply by preserving the ratios of the stereotaxic coordinates. To transfer these ratios to the *PCD* brains, which are smaller, the stereotaxic coordinates were recalculated from a new reference system whose origin was the geometric center of the OB. Similar injection sites could therefore be estimated as fractions of the rostrocaudal and mediolateral dimensions. Glass micropipettes with tip diameters of 10–25 μm were filled with 10% (w/v) BDA in distilled water. The tracer solution was delivered iontophoretically using 5 μA positive current pulses (7 sec on /7 sec off) for 3 min. The micropipette was left in place for 10 min after the injection and then withdrawn gently.

Seven days after the injection, the animals were sacrificed. They were anaesthetized with a solution composed of ketamine (120 μg/ g b.w.) and xylazine (10 μg/ g b.w.) intraperitoneally (i.p.) and perfused through the ascending aorta, first with saline for 1 min and then with 150 ml of fixative containing 4% (w/v) depolymerized paraformaldehyde and 0.2% (w/v) picric acid in 0.1 M phosphate buffer (PB), pH 7.4. The brains were removed, cut into two blocks, and immersed in the same fixative solution for 2 hr at room temperature. Brains were then rinsed carefully in PB and cryoprotected with 30% (w/v) sucrose in PB overnight at 4°C. After this, 40 μm coronal serial sections were obtained with a freezing microtome and collected in PB in six alternating series. The transported BDA was visualized using the avidin–biotin–peroxidase procedure, following the manufacturer's specifications (ABC kit, Vector, Burlingame, CA). Peroxidase was developed by incubating the sections in a solution of 0.05% diaminobenzidine tetrahydrochloride (DAB) and 0.003% (v/v) H_2O_2 in 0.2 M Tris-HCl buffer, pH 7.6. Sections were rinsed in PB and mounted onto gelatin-coated slides. After drying, they were dehydrated through a graded alcohol series, cleared with xylene, and coverslipped with Entellan (Merck, Darmstadt, Germany).

Controls were carried out by incubating some sections exclusively with DAB and H_2O_2 in Tris buffer, to exclude the presence of endogenous peroxidase. No staining was found. For anatomic reference, alternate sections were

counterstained for Nissl, labeling with 0.25% thionin. All sections were dehydrated, cleared, and coverslipped with Entellan.

The sections were examined and the areas containing labeled fibers or neuronal bodies were photographed with an Olympus Provis AX70 microscope and drawn with a *camera lucida*. The anatomic identification of the stained structures was based on atlases of the mouse brain by Franklin and Paxinos (1997) and Hof et al. (2000). For this study, only the animals with small tracer injections centered in the mitral cell layer of the OB were considered (Fig. 1).

Quantitative and Statistical Analyses

Despite of the known differences due to the intrinsic variability of the tracer injection method, we considered only the highly significant differences that were consistent in all the mutant animals studied and were differentiated consistently from those seen in the controls. To ensure the success of this, the analyses were carried out by observers who were blind to the identity of the animals. Moreover, as a result of its noteworthy differences the results regarding the AON were quantified and analyzed statistically. Quantification of retrogradely-labeled neurons in the ipsilateral AON and estimations of subdivision areas were carried out using Neurolucida software (MicroBrightField, Williston, VT). The densities of positive cells in each subdivision of the AON of both experimental groups, *PCD* and control, were calculated and statistical differences were assessed with the Mann-Whitney test. The level of significance was set at $P < 0.05$.

RESULTS

The results described below were obtained in selected cases (4 animals/group) in which the injection site was centered in the region of the mitral cell layer (Fig. 1) and did not present significant size differences between similar rostro–caudal levels. Moreover, all these cases were absolutely confined to the OB, and the tracer did not spread beyond its limits. For better understanding, the results are divided into several sections: anterior olfactory nucleus, lateral olfactory tract, rostromedial olfactory cortex, lateral olfactory cortex, and anterior commissure (ACO). It is important to note that when talking about differences in the amount of positive structures, we are only referring to qualitative observations in all areas, excepting the AON, where we did count the number of positive cells, because quantitative data were considered indispensable.

Anatomic Considerations

The size of the OB in *PCD* mice is considerably smaller than in control animals (Mullen et al., 1976), due mainly to the loss of mitral cells. Theoretically, similar injections could recruit more axons and label more cells retrogradely in *PCD* mice. However, except for the AON (see below), there were no important differences between both experimental groups in the amount of retrogradely-labeled neurons among the regions projecting to the OB. This observation is significant because it

means that the results from both the control and mutant mice can be compared directly.

Anterior Olfactory Nucleus

The AON regulates sensory inputs to the olfactory system by means of projections to both the ipsilateral and contralateral OB (De Olmos et al., 1978; Haberly and Price, 1978a; Schoenfeld and Macrides, 1984; Brunjes, 1994). It is also involved in the interhemispheric processing of olfactory information (Cleland and Linster, 2003). In both experimental groups (control and *PCD* mice), fibers containing tracer were observed in the superficial part of the plexiform layer of all subdivisions of the ipsilateral AON (Fig. 2). However, the fiber density was much lower in the mutant than in the control mice (Fig. 2). In the contralateral AON of the controls, labeled fibers were also observed, but they were scarce and scattered. It is worth noting that olfactory bulb output neurons do not project contralaterally (Switzer et al., 1985). Accordingly, the labeled fibers found in the contralateral AON of the control mice must belong to intrinsic neurons of this region projecting to the contralateral OB, where they would uptake BDA retrogradely. In *PCD* mice, no positive structures, either fibers or neurons, were found in the contralateral hemisphere.

Retrogradely-labeled neurons were found in both AON of the control mice. In the ipsilateral AON, they were located in all its subdivisions, excluding the *pars externa* (Fig. 2A). Interestingly, the *pars externa* was the subdivision with the highest amount of positive neurons in the contralateral AON. In the *PCD* mice, the total number of retrogradely stained neurons in the ipsilateral AON was clearly higher than in the control animals (Table I, Figs. 2D, 3A). Likewise, the density of positive cells was higher in all subdivisions of the *PCD* ipsilateral AON (Table II, Fig. 3B). In contrast to the observations in the control animals, labeled neurons were seen in all the ipsilateral AON subdivisions of the *PCD* mice, including the *pars externa* (Fig. 2D).

Lateral Olfactory Tract

Figures 4–6 show *camera lucida* drawings of the hemispheres ipsilateral to the BDA injection of a control and a *PCD* mouse. In mammals, the lateral olfactory tract (LOT) courses along the ventrolateral surface of the basal forebrain, giving off collaterals within the secondary olfactory structures. In the control mice, positive fibers were detected all along the LOT (Figs. 4B–H, 6I), decreasing as the projections extended more caudally. The highest density of labeled fibers was observed in the central region of the LOT, near to the rostral most portion of the piriform cortex (Fig. 7A). In the LOT, we identified different types of tracer-containing fibers, including thick fibers, thin fibers without varicosities, and thin fibers with varicosities.

In the *PCD* mice, the size of the LOT and the amount of labeled fibers in that tract were much smaller than in the control mice (Fig. 7C). In addition, the caudal
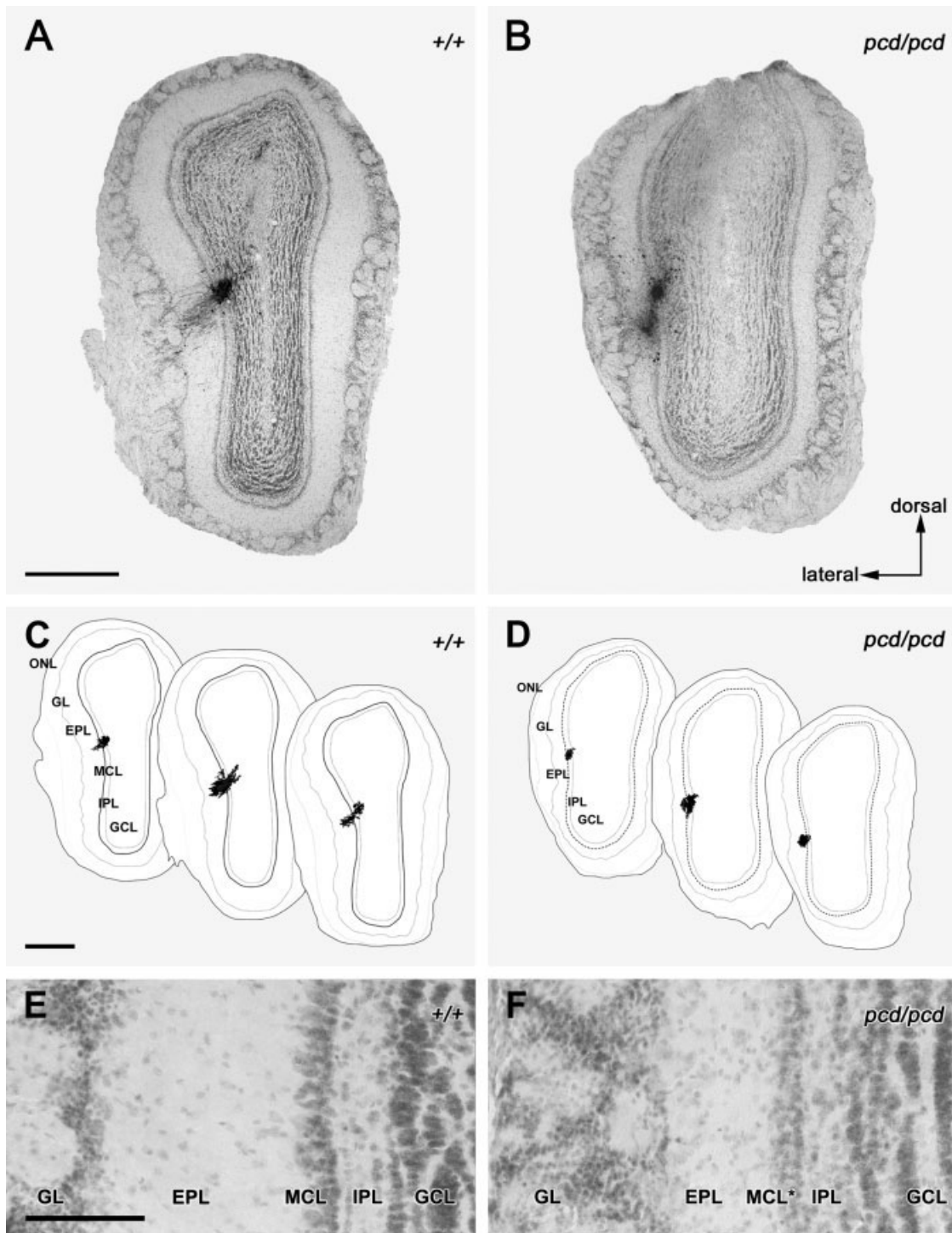
Fig. 1. Coronal sections of the mouse olfactory bulb showing the BDA tracer injection sites counterstained with the Nissl technique. Injection sites reach the mitral cell layer and are completely confined to the OB. **A:** Control mouse. **B:** *PCD* animal. **C,D:** Series of consecutive sections showing the spread of a typical injection site from a control and a mutant mouse, respectively. D: Discontinuous line is where the mitral cell layer should be. **E,F:** Magnifications showing the OB laminar organization from a control and a *PCD* mouse respectively. F: No mitral cell layer (MCL*, where it should be located) and the granule cell layer is smaller than in a control mouse. EPL, external plexiform layer; GCL, granule cell layer; GL, glomerular layer; IPL, internal plexiform layer; MCL, mitral cell layer; ONL, olfactory nerve layer. Scale bars = 500 μm (A,B); 100 μm (C–F).

decrease observed in the control mice was much more pronounced in the *PCD* mice and began at more rostral levels. We also found all of the types of positive fibers described previously, although the thick ones were very

TABLE I. Total Number of Retrogradely-Labeled Neurons in the Ipsilateral AON of *PCD* Mice Is Clearly Higher Than in Control Mice

	Control (n = 4)	*PCD* (n = 4)	*P* for Mann–Whitney test (control vs. *PCD*)
Ipsilateral AON	22.75 ± 7.33	173.75 ± 42.82	0.021★
Contralateral AON	12 ± 3.34	0	0.013★

Quantity of positive cells in the ipsilateral AON of both experimental groups (control and *PCD*). Data represent means ± SEM. AON, anterior olfactory nucleus; PCD, Purkinje cell degeneration.
★*P* < 0.05 control vs. *PCD* data.
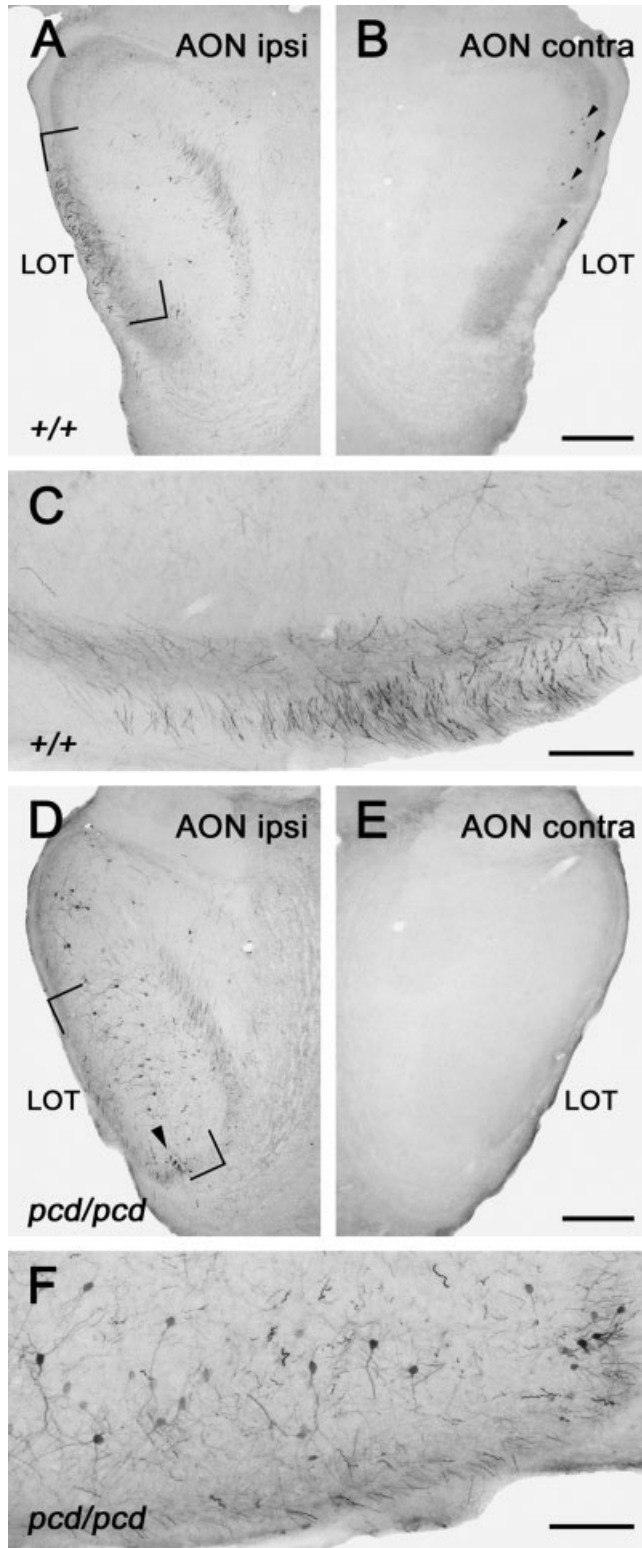
rare (Fig. 7B,D). The other types of fibers did not show important differences in comparison with the control animals.

Rostromedial Olfactory Cortex

We studied the results for the *taenia tecta*, the anterior hippocampal continuation, the *indusium griseum*, and the olfactory tubercle. Like Shipley and Adamek (1984), we considered the *taenia tecta* only as the ventral subdivision of the homonymous structure described by Haberly and Price (1978a,b). In the control mice, fibers containing BDA were observed to run from the plexiform layer of the AON into the most superficial part of the plexiform layer of the whole of this structure. They were less numerous than in the plexiform layer of the AON, but they extended throughout this region of the *taenia tecta*. In the *PCD* mice, however, they were not distributed evenly throughout the plexiform layer and were clearly fewer in number than in the control animals (Figs. 4E,F, 5E,F). Retrogradely-labeled neurons were found in this area in both the control and the mutant animals. The neurons were very scarce and their labeling was always weak (data not shown).

In the anterior hippocampal continuation, positive fibers were only found in some of the control mice, and they were very scarce and confined to the most superficial part of its plexiform layer. Labeled neurons were seen occasionally in the rostral most part of this region in both phenotypes, but they were not detected in all cases studied

Fig. 2. Coronal sections of the anterior olfactory nucleus (AON) from a control mouse (**A–C**) and a *PCD* mouse (**D–F**) in which injected tracer is visualized histochemically. A: Ipsilateral AON with a huge quantity of labeled fibers seen in the external part of the plexiform layer, together with a few retrogradely-labeled neurons. B: Contralateral AON with retrogradely-labeled neurons (black arrowheads). C: Magnification from (A) showing positive fibers in both Layer I of the AON and the lateral olfactory tract (LOT). D: Ipsilateral AON from a *PCD* mouse, where retrogradely-labeled neurons are more numerous than in controls (A), some of them located in the *pars externa* (black arrowhead). F: Magnification from (D). Within the contralateral AON from a *PCD* mouse (E), no positive elements are detected. Scale bars = 250 μm (A,B,D,E); 100 μm (C,F).

A

Total number of retrogradely labelled cells in the AON of control and PCD mice

B

Density of retrogradely labelled cells in each subdivision of the ipsilateral AON
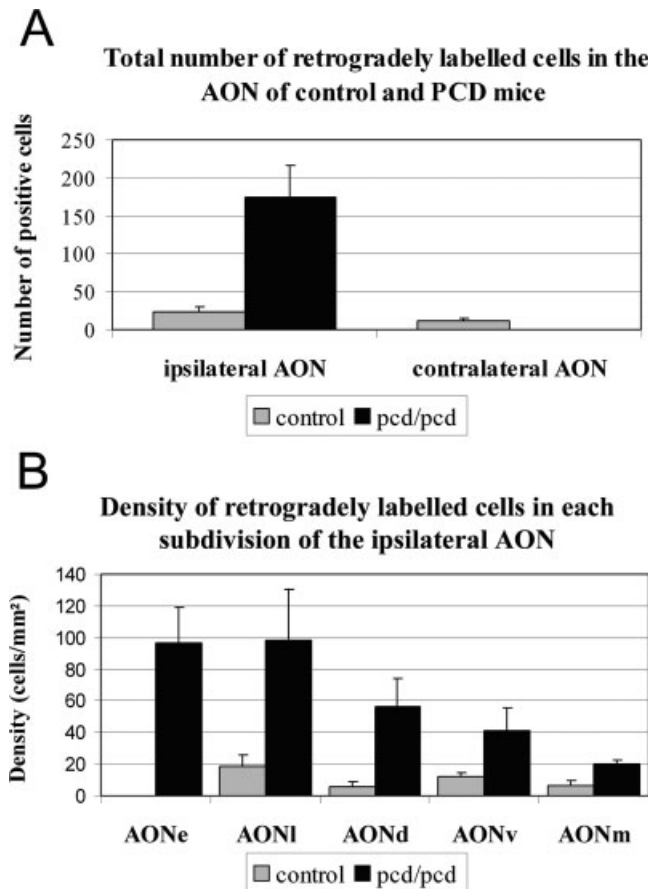

Fig. 3. Important differences are seen in the quantity of neurons projecting to the OB from the ipsilateral AON after mitral cell neurodegeneration. **A** represents the quantitative analysis of total positive cells in both the ipsilateral and the contralateral AON of the control and *PCD* mice, the latter exhibiting much higher numbers in the ipsilateral AON. Note that there are no positive cells in the *PCD* contralateral AON. **B** shows the quantitative analysis of the density of retrogradely-labeled cells in each subdivision of the ipsilateral AON of both experimental groups. All subdivisions showed significant differences between control and *PCD* mice. AON*e*, pars externa; AON*d*, pars dorsalis; AON*l*, pars lateralis; AON*v*, pars ventralis; AON*m*, pars medialis.

and their staining was very weak. No labeled fibers or neurons were observed in the *indusium griseum* of any of the animals.

Finally, in the olfactory tubercle of the control mice, positive fibers extending throughout this structure were seen. Similarly to the structures described above, the labeled elements were also restricted to the external most part of the plexiform layer. They were not very abundant and their numbers decreased caudally (Fig. 4E,F). The density of positive fibers in the olfactory tubercle was lower than that observed in the same region of the AON. Regarding retrograde labeling, we did not find any neurons projecting to the olfactory bulb from this area in the control or the *PCD* mice. Further, in the *PCD* mice a

TABLE II. Density of Positive Cells in Each Subdivision of the *PCD* Ipsilateral AON Is Compared With Controls

Ipsilateral subdivisions	Control (n = 4)	*PCD* (n = 4)	*P* for Mann–Whitney test (control vs. *PCD*)
AON*e*	0	96.67 ± 22.63	0.014★
AON*l*	18.60 ± 7.21	98.43 ± 32.20	0.043★
AON*d*	5.35 ± 3.50	56.25 ± 17.70	0.020★
AON*v*	11.95 ± 2.57	40.88 ± 14.73	0.043★
AON*m*	6.77 ± 2.76	20.15 ± 2.27	0.021★

Density of retrogradely labeled neurons in each subdivision of the ipsilateral AON of both experimental groups (control and *PCD*). Data represent means ± SEM. AON, anterior olfactory nucleus; AON*e*, *pars externa*; AON*l*, *pars lateralis*; AON*d*, *pars dorsalis*; AON*v*, *pars ventralis*; AON*m*, *pars medialis*; PCD, Purkinje cell degeneration.
★$P < 0.05$ vs. control data.

slight reduction in the density of positive fibers was detected as compared to the control animals (Fig. 5E,F).

Lateral Olfactory Cortex

The lateral olfactory cortex includes the piriform, the periamygdaloid, the entorhinal cortices, and the anterior cortical nucleus of the amygdaloid complex (Shipley et al., 1996). In both phenotypes, fibers containing neurotracer were located along the external most part of the plexiform layer of the piriform cortex (Fig. 7A,C); the nearer to the LOT, the more abundant were the positive fibers. These fibers had a small diameter mainly and few varicosities. In the control mice, the density of these fibers was fairly similar throughout this region, although it decreased slightly in the caudal direction. However, these BDA-labeled fibers were very scarce in the *PCD* mice. Further, they were not present throughout the entire piriform cortex in the mutant mice. A decrease in the amount of labeled fibers was also detected caudally along this region, but it was more marked in the *PCD* animals as compared to the controls. Moreover, this decrease began more rostrally in the mutants than in the wild-type mice. Together with the AON, the piriform cortex exhibited the most extensive field of retrograde labeling in both experimental groups, especially the part closest to the LOT (Fig. 7A,C). We did not observe significant differences in the amount of these positive neurons between Layers II and III. The density of these retrogradely-labeled neurons decreased caudally, and more sharply than the decrease in positive fibers. No significant changes concerning the retrograde labeling were detected on comparing the control and *PCD* mice.

In the periamygdaloid cortex, the distribution of fibers containing BDA was similar to that seen in the piriform cortex. However, they were not as abundant as in the piriform cortex. Despite this, they were observed throughout this structure in the control mice (Figs. 4H, 6I,J). In the *PCD* mice they were very scarce and did not extend throughout the whole plexiform layer (Figs. 5H,
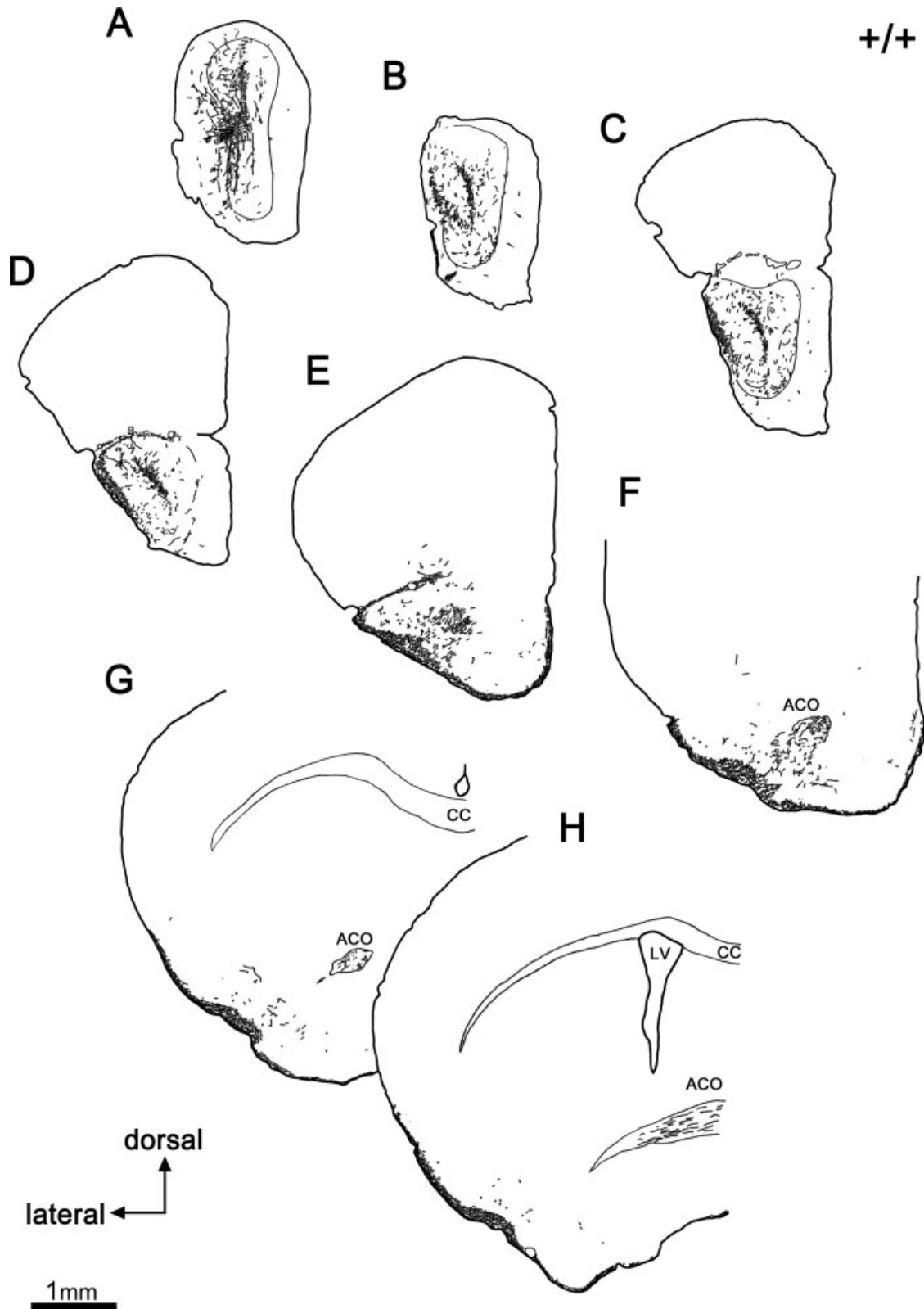
Fig. 4–6. Camera lucida drawings of selected coronal sections from the mouse brain. BDA tracer was injected iontophoretically into the OB of control mice (Case 03403; Figs. 4 and 6 up) or *PCD* mice (Case 03410; Figs. 5 and 6 down). In all figures, (A) is the rostral most region, and (N) is the caudal most one for the control case, whereas (T) is the caudal most one for the mutant case. Drawings show the structures containing tracer in the hemisphere ipsilateral to the injection. Note that the labeling reaches more caudal regions in the wild-type animal. ACO, anterior commissure; CC, corpus callosum; LV, lateral ventricle. Scale bar = 1 mm.

pcd/pcd

A

B

C

D

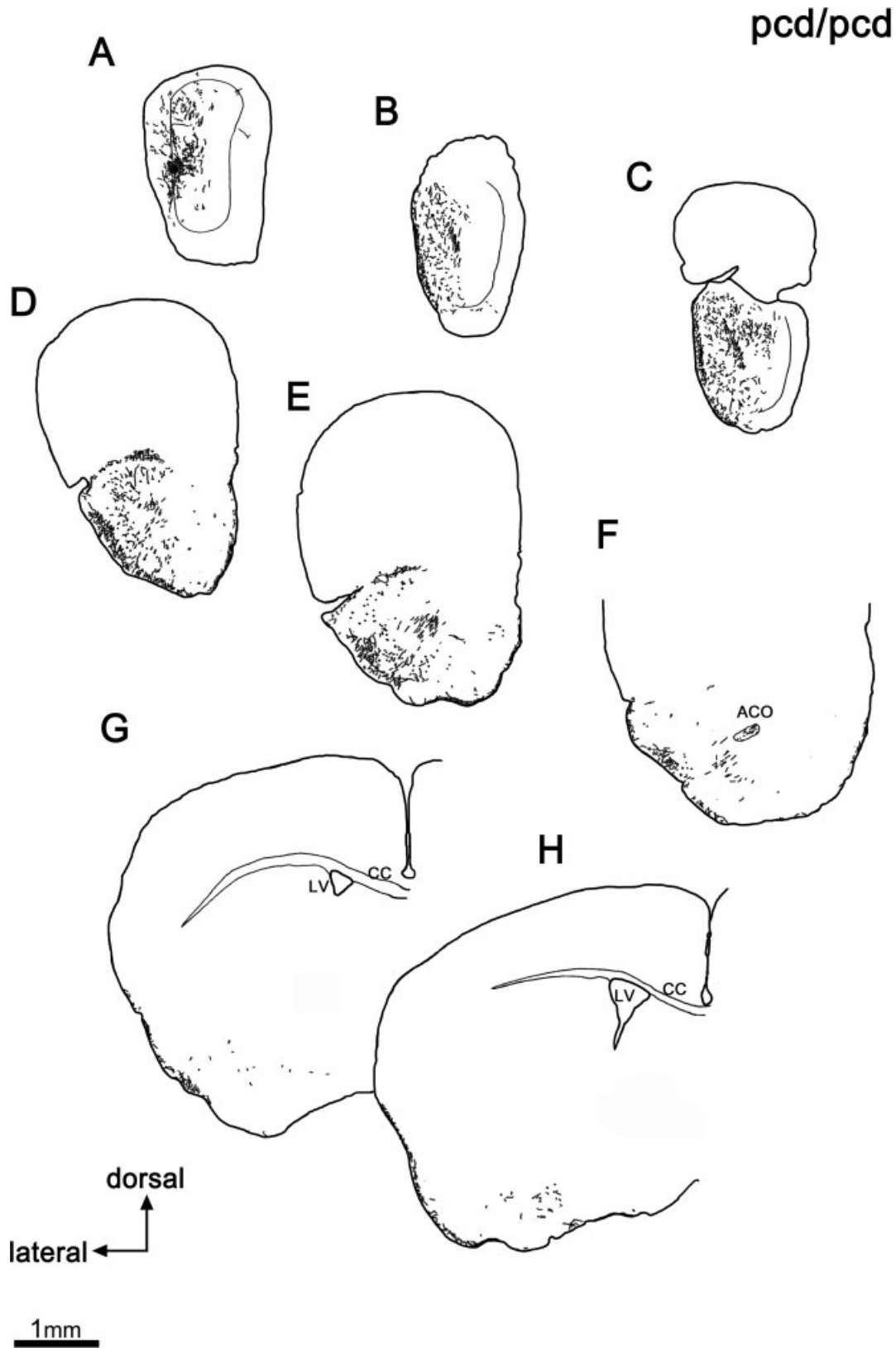E

F

ACO

G

CC

LV

H

LV   CC

dorsal

lateral

1mm
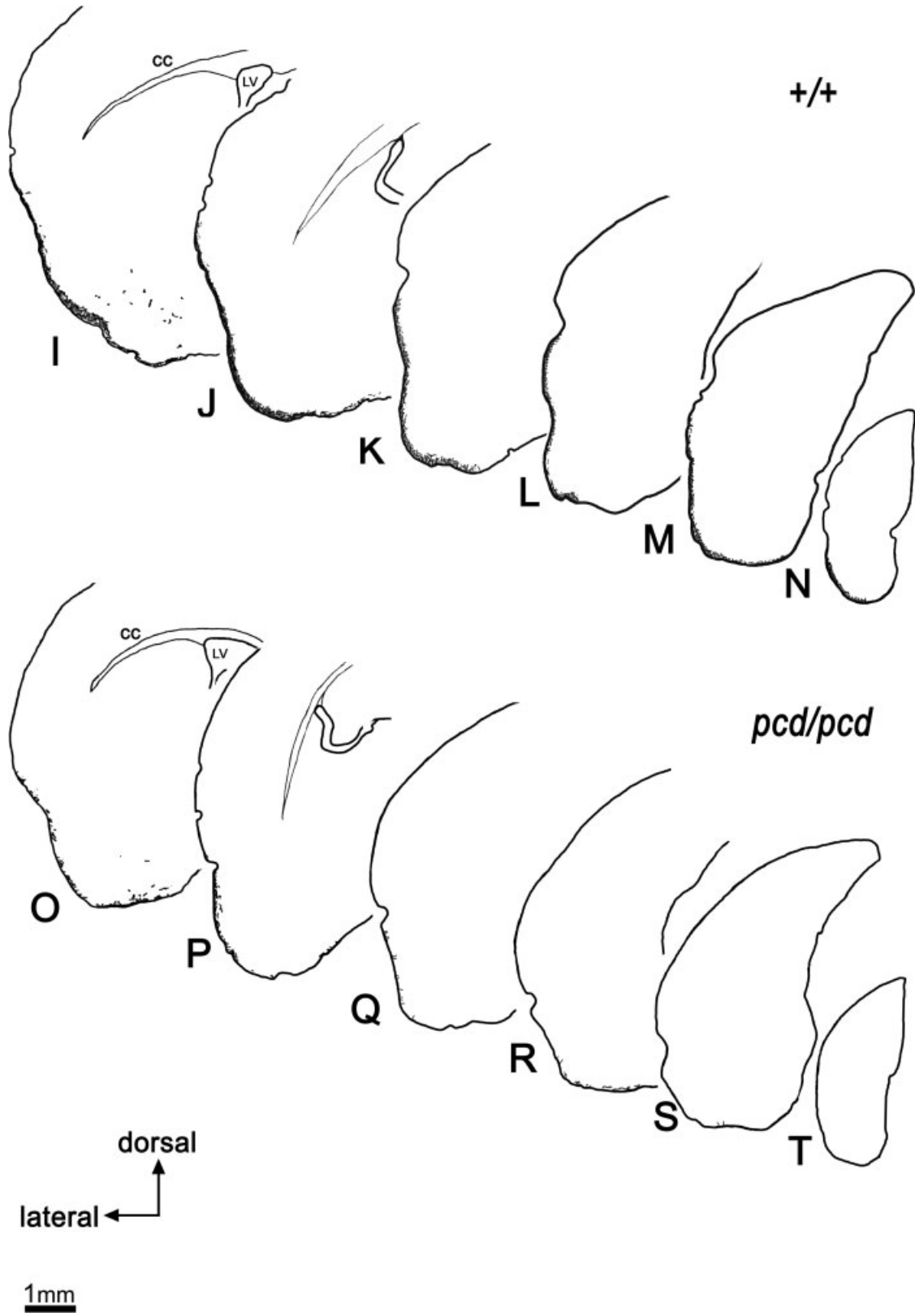
Figure 5. (Legend on page 2413.)
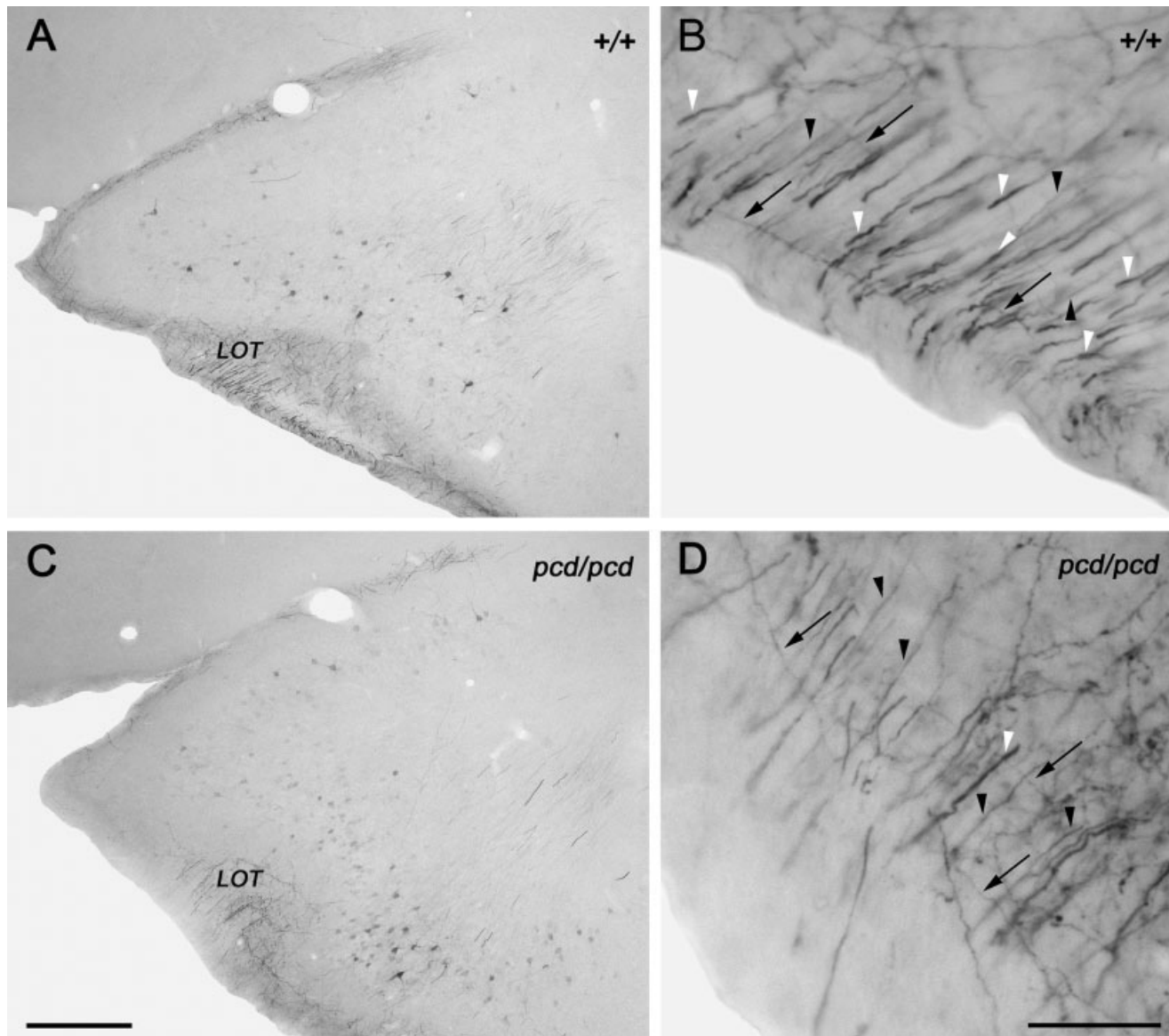
Figure 6. (Legend on page 2413.)

Fig. 7. Coronal sections of the piriform cortex and the lateral olfactory tract from a control mouse (**A,B**) and a *PCD* mouse (**C,D**) where tracer is visualized histochemically. A,C: Positive fibers are located within the external most part of the plexiform layer, but their density is lower in the mutant mice. No significant changes in the number of positive neurons are seen on comparing both experimental groups. In the LOT, different types of tracer-containing fibers can be identified: thick fibers (white arrow point), thin fibers with (black arrow) and without (black arrow point) varicosities. In *PCD* mice, the thick ones were very rare. Scale bar = 500 μm (A,C); 50 μm (B,D).

6O,P). Likewise, these few positive fibers did not reach the caudal limit of this cortex. In both groups of animals, no labeled neurons were found within the periamygdaloid cortex, apart from those belonging to both the anterior cortical nucleus of the amygdaloid complex and to the lateral olfactory tract nucleus. In these nuclei, no significant differences between the control and *PCD* mice were observed. The positive fibers in these nuclei had similar features to those seen in the periamygdaloid cortex, although they were rare. Labeled fibers with and without varicosities were seen in this region.

The entorhinal cortex is located caudal to both the piriform and periamygdaloid cortices and it is divided into the medial, lateral and intermediate divisions. The lateral entorhinal cortex is the caudal most target of olfactory bulb axons (Heimer, 1968; Price, 1973; Scalia and Winans, 1975; Davis et al., 1978). As occurred in the structures described above, positive fibers were restricted to the external most part of the plexiform layer (Fig. 6J–N). In the control mice, the labeling in Layer I of the piriform cortex continued caudally into the lateral entorhinal cortex. Some of these fibers had pleomorphic
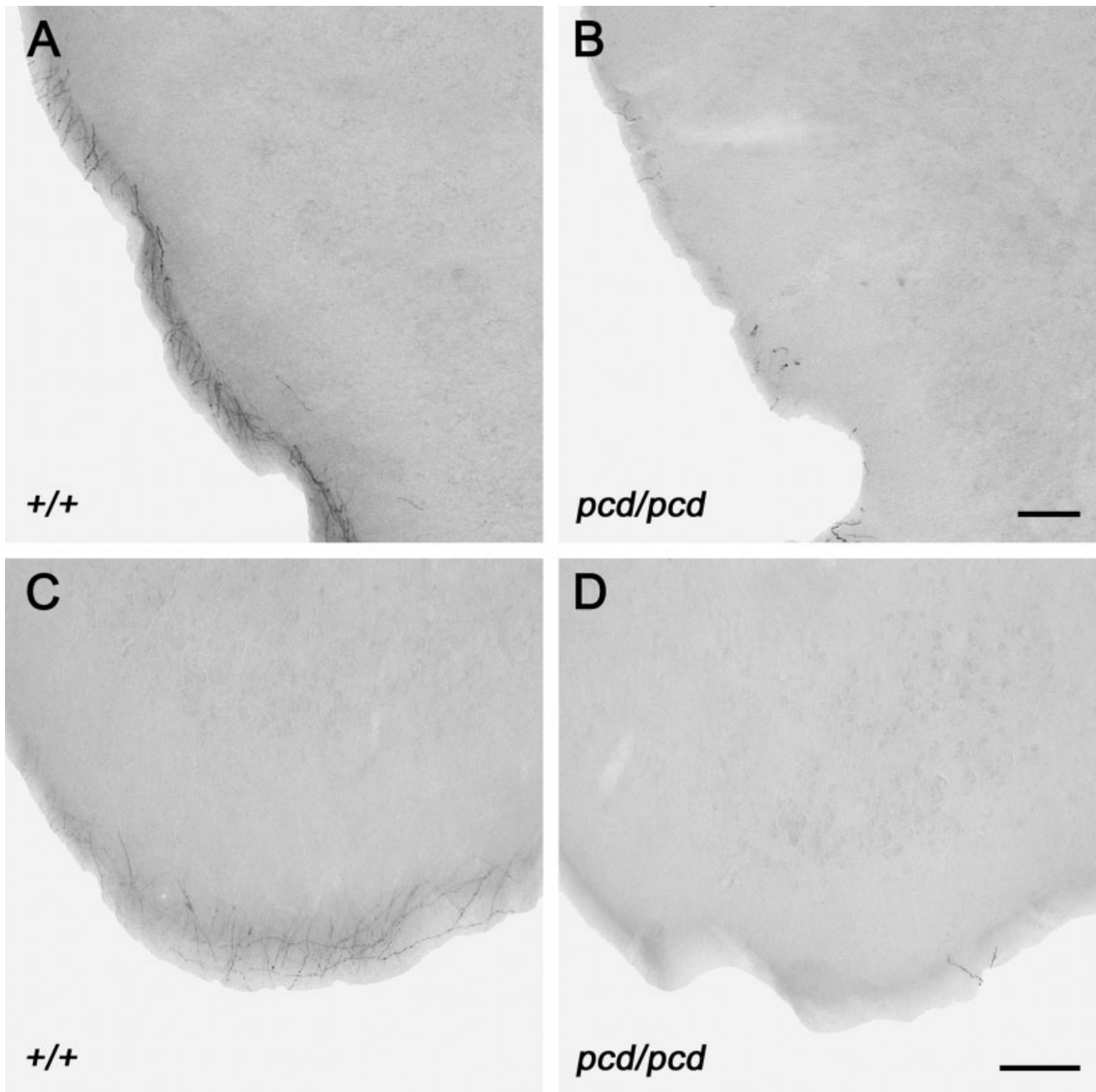
Fig. 8. Coronal sections of the brain through the rostral most lateral entorhinal cortex (**A,B**) and the caudal most lateral entorhinal cortex (**C,D**) from a control mouse (A,C) and a *PCD* mouse (B,D), where injected tracer is visualized histochemically. Positive fibers are much more abundant in control mice than in *PCD* mice. In the caudal most region of *PCD* mice they are almost completely absent. Scale bar = 50 μm (A,B); 100 μm (C,D).

varicosities, and their highest density was seen in the central area of this structure, decreasing caudally. Despite this, fibers containing BDA were always found up to the caudal most part of the lateral entorhinal cortex (Fig. 6N). The BDA-labeled elements in this region were very scarce in the *PCD* mice (Fig. 6P–T), and they only appeared in some mutants. When present, most of these fibers were restricted to the rostral most part of the lateral entorhinal cortex. Similarly to the piriform cortex, the labeled fibers were confined to the external most part of Layer I in the lateral entorhinal cortex (Fig. 8). The few positive fibers found more caudally were always located in the ventral part of the cortex, the dorsal part not being reached, as in the control mice (Fig. 6Q–T). Retrograde labeling in the neurons of this region was rare and was not observed in all cases studied in both experimental

groups. When present, retrograde labeled neurons were always located in rostral parts close to the piriform cortex and their staining was always weak.

Anterior Commissure

This structure is one of the main projection pathways of the olfactory system. Although it does not contain any collateral of mitral or tufted cell axons, it is an important component of the olfactory system because axons arising from both the piriform cortex and the AON, target areas of olfactory output neurons, decussate along this tract (Price, 1973; Devor, 1976; Haberly and Price, 1977, 1978a,b; Luskin and Price, 1983). In the control mice, the ACO contained positive fibers in both hemispheres (Fig. 9A–C). These fibers were both thick and thin and were located throughout this structure. However, in the PCD mice only fibers containing tracer in the rostral most part of the ACO of the ipsilateral hemisphere were observed. Additionally, the ACO was very reduced in the mutant animals, being observed only in the rostral most part of the forebrain. Positive fibers were thin mainly and much less abundant than in the controls. In contrast to the control mice, the caudal most part of this structure, where fibers normally cross to the other hemisphere, was not observed in any of the PCD mice (Fig. 9D–F).

DISCUSSION

The present results offer the first evidence in the mouse about the different projection patterns from mitral and tufted cells of the OB. The level of resolution of this olfactory tracing has not been previously reported. Although BDA neurotracer has been used successfully in hodologic studies in other regions of the mammalian brain (Reiner et al., 2000), this is the first time it has been used in olfactory connectivity. Our study also show very significant histologic changes in the olfactory pathway after mitral cell neurodegeneration in the PCD mutant mouse. This reorganization must be determined by both an increase in the centrifugal input strength from the ipsilateral AON to the OB and a loss of bilaterality related to both ACO degeneration and a lack of interhemispheric connections.

Anterior Olfactory Nucleus

Because the olfactory output neurons project ipsilaterally to the plexiform layer of all subdivisions of the ipsilateral AON (Price, 1973; Scott et al., 1985), the lower density of tracer-containing fibers in PCD mice must be a direct consequence of mitral cell degeneration. Regarding the retrogradely-labeled neurons, important divergences were seen on comparing both experimental groups. The mutant mice exhibited many more neurons projecting to the OB from the ipsilateral AON. We suggest that a higher number of BDA-filled neurons would reflect an increase in the centrifugal input strength to the OB from the ipsilateral AON, due probably to loss of part of the olfactory afferences to this region. This phenomenon could be related to odor-deprived adult rats, where experimental
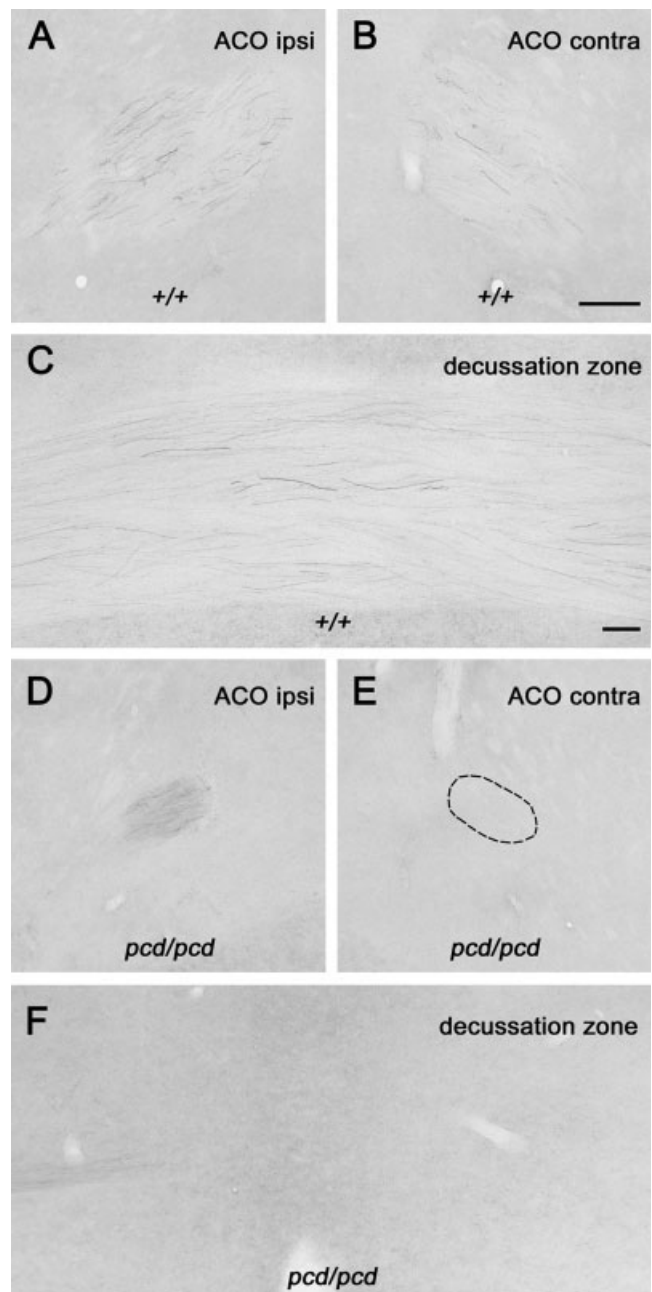

Fig. 9. Coronal sections of the brain through the anterior commissure (ACO) region from a control mouse (**A–C**) and a PCD mouse (**D–F**), where tracer is visualized histochemically. Rostral areas of the ACO from the ipsilateral (A,D) and the contralateral hemisphere (B,E) are shown, whereas enlarge-captions depict the caudal most areas (C,F). The ACO is much larger and has more positive fibers in the controls than in the mutants. In the control animals, positive fibers are more abundant in the ipsilateral (A) than in the contralateral hemisphere (B). However, in the PCD mice no positive fibers are detected in the contralateral hemisphere (E). C,F: Decussation zone, the caudal most region of the ACO, where fibers cross to the other hemisphere. This region was not readily distinguishable in the PCD mice studied (F). Scale bars = 100 μm (A,B,D,E); 50 μm (C,F).

unilateral naris occlusion results in important anatomic and neurochemical changes in the AON (Barbado et al., 2002).

Another important result is the absence of labeled elements throughout the contralateral hemisphere in the *PCD* mice. The lack of positive neurons in the contralateral AON of the *PCD* mice is related directly to anterior commissure degeneration (see below) and the loss of interhemispheric connections. We infer that the lack of information provided usually by mitral cells would elicit a reorganization of the OB–AON interconnections. Moreover, the absence of contralateral inputs seems to be compensated through the increase in the centrifugal input strength from the ipsilateral AON.

Unlike what was seen in the control mice, we found labeled neurons in the *pars externa* of the ipsilateral AON. This region has been described to hold only contralateral projections from the OB (Shipley et al., 1996; Brunjes et al., 2005), in agreement with our findings in control mice. Accordingly, the presence of neurons in the *pars externa* of the AON that project ipsilaterally seems to be another piece of evidence supporting an important reorganization. These results show a strong and selective capacity for neuronal plasticity in the adult olfactory system after selective loss of neuronal elements.

Lateral Olfactory Tract

Our results in the LOT are a useful direct anatomic confirmation in the mouse of previous electrophysiologic (Scott, 1981) and electron microscopy (Bartolomei and Greer, 1998) studies suggesting that mitral cells have larger axons than tufted cells.

In the LOT of both groups of animals, we observed a heterogeneous population of positive fibers. These belonged not only to centrifugal afferences to the OB but also to olfactory projection neurons, because BDA labels neurons both retrogradely and anterogradely, and hence the fibers observed in the LOT must contain both elements. Despite this, we consider that the only difference between both experimental groups would be related to the thick fibers, and therefore they must be mitral cell axons because they were quite scarce in the *PCD* mice, in agreement with the very few remaining mitral cells surviving in the OB. At P120, both mitral cell somata and their axons had not disappeared completely because the degeneration process takes place gradually, and at that time-point this neurodegeneration is not entirely complete, although surviving mitral cells are rare (Baker and Greer, 1990) (personal observations). The remaining positive fibers, which were fairly similar in both experimental groups, could be tufted cell axons because they persisted similarly in both experimental groups, or centrifugal axons projecting to the OB through the LOT. With the different aspects addressed in this study, we are unable to discern the origin of these thin labeled fibers. Because there is no difference between *PCD* and control mice, this should not influence the results of our study. We also observed that the LOT disappeared in more rostral levels

in the *PCD* mice. This confirms, in the mouse, the hypothesis proposed for the rat, suggesting that mitral cell axons project to more caudal parts of olfactory cortex than the tufted cell axons.

Rostromedial Olfactory Cortex

The results for the *PCD* mice indicated that most of the afferences to the *taenia tecta* from the OB arose from mitral cells, which are missing in these animals, and therefore that tufted cells innervate this region poorly. Regarding the anterior hippocampal continuation and *indusium griseum*, we were unable to confirm accurately the existence of efferences from the OB to these structures described previously (De Olmos et al., 1978; Wyss and Sripanidkulchai, 1983; Shipley and Adamek, 1984; Shipley et al., 1996). This divergence with the results of previous studies can be explained in terms of the methodologic basis of the injection. Shipley and Adamek (1984) described positive fibers in both the anterior hippocampal continuation and the *indusium griseum* only in cases where the injection site covered a large proportion of the OB. Moreover, in those cases the tracer was injected by hydraulic pressure, risking more widespread staining than after iontophoretic injections. Our results concerning retrogradely-labeled neurons in these structures in the mouse were fairly similar to those reported in rat in previous studies. Finally, in the olfactory tubercle, the reduction in the density of positive fibers in the *PCD* mice was less marked than in the *taenia tecta*. We therefore assume that both mitral and tufted cells project to this region in a similar manner.

Lateral Olfactory Cortex

Our results support the differential distribution of mitral and tufted axons described in other rodents. Our method affords meaningful results, completing those described previously in the rat. To date, it has been difficult to discern accurately whether tufted cell axons innervate regions as caudal as those innervated by mitral cells. The present analysis of *PCD* mouse projections sheds some light on this issue. We consider that in the few cases of mutant mice where scarce fibers containing BDA were observed in caudal regions they belonged to the few surviving mitral cells at this stage because the degenerative process is not complete at P120. Tracer injections in older animals would clarify this question, but both mortality and morbidity increase exponentially when older *PCD* mutants undergo surgery. The efferences from the lateral olfactory cortex to the OB seen in our studies are in accordance with those described in previous ones.

Anterior Commissure

We observed a strong reduction in the size of the ACO in P120 *PCD* mice, a considerably younger age than the 6–7-month-old animals, analyzed by Baker and Greer (1990). The mechanism underlying this extinction in *PCD* mice is unknown, but two alternative

explanations could be advanced: the reduction would either take place independently of mitral cell degeneration or would be a consequence of said primary mitral cell neurodegeneration. The first hypothesis would imply that the *PCD* mutation would exert broader effects than those hitherto described (Mullen et al., 1976; Fernández-González et al., 2002). In the second hypothesis, the primary degeneration would elicit changes in the targets of the degenerated mitral cells in both the AON and the piriform cortex that would affect their contribution to the tract, leading to the disappearance of the latter. Regarding this second hypothesis, two possibilities could be proposed: 1) a loss of neuronal subpopulations in the AON or in the piriform cortex would take place, although this seems unlikely because no differences have been found on examining these regions; or 2) the absence of the commissural pathway would reflect the loss of only one system of axon collaterals: those that arise from neurons from both the AON and the piriform cortex. This explanation would be unlikely because the commissural system axons synapse onto granule cells, which are not affected in *PCD* mice, but not directly on mitral cells (Luskin and Price, 1983; Mori, 1987). Likewise, a possible trans-synaptic effect via granule cells has also been ruled out, because tufted cells, not directly affected in *PCD* mice, receive a similar input from granule cells (Greer and Halász, 1987; Baker and Greer, 1990).

To date, the time window where the ACO fades in *PCD* mice is unknown. We observed that *PCD* mice (4 months) younger than those studied previously (6–7 months) (Baker and Greer, 1990) show a lower density of fibers containing tracer within the ACO than that of control mice, and that they were always restricted to the rostral most region of this tract in the ipsilateral hemisphere. Such fibers must belong to neurons located in the ipsilateral hemisphere but that exhibit collaterals to both the injected OB (from where they had incorporated the BDA) and the ACO, through which they would transport the BDA anterogradely. However, further studies on the axon endings within the rostral anterior commissure in *PCD* mice should attempt to determine whether those collaterals travel along the tract when the collapse of the structure begins, or whether they represent a sprouting process that occurs after the degeneration of the tract has been accomplished. This labeling implies the existence of a complex transport system, designated collateral transport (Merchán et al., 1994).

This study shows that the *PCD* mouse shows a general decrease in the efferences from the OB to secondary olfactory structures, as expected. Additionally, the observed differences between the control and mutant mice definitively support the notion that mitral cell axons project to more caudal regions than tufted cell axons in the mouse. Finally, it confirms important results concerning histologic changes in the olfactory connections in relation to mitral cell degeneration. These changes are seen in both an increase in the ipsilateral afferences to the OB from the ipsilateral AON, reflecting a reinforcement in the ipsilateral centrifugal input strength from this area, and a lack of bilaterality linked to the loss of the ACO, and hence the absence of contralateral connections. This reorganization of the olfactory pathway in the *PCD* mutant mouse shows clearly neural plasticity in adulthood.

REFERENCES

Baker H, Greer CA. 1990. Region-specific consequences of *PCD* gene expression in the olfactory system. J Comp Neurol 293:125–133.

Barbado MV, Briñón JG, Weruaga E, Porteros A, Arévalo R, Aijón J, Alonso JR. 2002. Changes in immunoreactivity to calcium-binding proteins in the anterior olfactory nucleus of the rat after neonatal olfactory deprivation. Exp Neurol 177:133–150.

Bartolomei JC, Greer CA. 1998. The organization of piriform cortex and the lateral olfactory tract following the loss of mitral cells in *PCD* mice. Exp Neurol 154:537–550.

Brunjes PC. 1994. Unilateral naris closure and olfactory system development. Brain Res Rev 19:146–160.

Brunjes PC, Illig KR, Meyer EA. 2005. A field guide to the anterior olfactory nucleus (cortex). Brain Res Rev 50:305–335.

Cleland TA, Linster C. 2003. Central olfactory structures. In: Doty RL, editor. Handbook of olfaction and gustation. Philadelphia: Marcel Dekker. p 165–180.

Davis BJ, Macrides F, Youngs WM, Schneider SP, Rosene DL. 1978. Efferents and centrifugal afferents of main and accessory olfactory bulbs in hamster. Brain Res Bull 3:59–72.

De Olmos J, Hardy H, Heimer L. 1978. The afferent connections of the main and the accessory olfactory bulb formations in the rat: an experimental HRP-study. J Comp Neurol 181:213–244.

Devor M. 1976. Neuroplasticity in the rearrangements of olfactory tract fibers after neonatal transection in hamsters. J Comp Neurol 166:49–72.

Fernández-González A, La Spada AR, Treadaway J, Higdon JC, Harris BS, Sidman RL, Morgan JI, Zuo J. 2002. *Purkinje cell degeneration* (*PCD*) phenotypes caused by mutations in the axotomy-induced gene, *Nna1*. Science 295:1904–1906.

Franklin K, Paxinos G. 1997. The mouse brain in stereotaxic coordinates. San Diego: Academic Press.

Greer CA, Shepherd GM. 1982. Mitral cell degeneration and sensory function in the neurological mutant mouse *Purkinje cell degeneration* (*PCD*). Brain Res 235:156–161.

Greer CA, Halász N. 1987. Plasticity of dendrodendritic microcircuits following mitral cell loss in the olfactory bulb of the murine mutant *Purkinje cell degeneration*. J Comp Neurol 256:284–298.

Haberly LB. 2001. Parallel-distributed processing in olfactory cortex: new insights from morphological and physiological analysis of neuronal circuitry. Chem Senses 26:551–576.

Haberly LB, Price JL. 1977. The axonal projection patterns of the mitral and tufted cells of the olfactory bulb in the rat. Brain Res 129:152–157.

Haberly LB, Price JL. 1978a. Association and commissural fiber systems of the olfactory cortex of the rat. I. Systems originating in the piriform cortex and adjacent areas. J Comp Neurol 178:711–740.

Haberly LB, Price JL. 1978b. Association and commissural fiber systems of the olfactory cortex of the rat. II. Systems originating in the olfactory peduncle. J Comp Neurol 181:781–807.

Heimer L. 1968. Synaptic distribution of centripetal and centrifugal nerve fibers in olfactory system of rat. An experimental anatomical study. J Anat 103:413–432.

Hof PR, Young WG, Bloom FE, Belichenko PV, Celio MR. 2000. Comparative cytoarchitectonic atlas of the C57BL/6 and 129/Sv mouse brains. Amsterdam: Elsevier.

Luskin MB, Price JL. 1983. The topographic organization of associational fibers of the olfactory system in the rat, including centrifugal fibers to the olfactory bulb. J Comp Neurol 216:264–291.

Macrides F, Schoenfeld TA, Marchand JE, Clancy AN. 1985. Evidence for morphologically, neurochemically and functionally heterogeneous classes of mitral and tufted cells in the olfactory bulb. Chem Senses 10:175–202.

Merchán MA, Saldaña E, Plaza I. 1994. Dorsal nucleus of the lateral lemniscus in the rat: concentric organization and tonotopic projection to the inferior colliculus. J Comp Neurol 342:259–278.

Mori K. 1987. Membrane and synaptic properties of identified neurons in the olfactory bulb. Prog Neurobiol 29:275–320.

Mullen RJ, Eicher EM, Sidman RL. 1976. *Purkinje cell degeneration*, a new neurological mutation in the mouse. Proc Natl Acad Sci USA 73:208–212.

Nagayama S, Takahashi YK, Yoshihara Y, Mori K. 2004. Mitral and tufted cells differ in the decoding manner of odor maps in the rat olfactory bulb. J Neurophysiol 91:2532–2540.

Pinching AJ, Powell TPS. 1971. The neuron types of the glomerular layer of the olfactory bulb. J Cell Sci 9:305–345.

Price JL. 1973. Autoradiographic study of complementary laminar patterns of termination of afferent fibers to olfactory cortex. J Comp Neurol 150:87–108.

Ramón y Cajal S. 1911. Histologie du système nerveux de l'homme et des vértebrés. Paris: Maloine.

Reiner A, Veenman CL, Medina L, Jiao Y, Del Mar N, Honig MG. 2000. Pathway tracing using biotinylated dextran amines. J Neurosci Meth 103:23–37.

Scalia F, Winans SS. 1975. Differential projections of olfactory bulb and accessory olfactory bulb in mammals. J Comp Neurol 161:31–55.

Schoenfeld TA, Macrides F. 1984. Topographic organization of connections between the main olfactory bulb and *pars externa* of the anterior olfactory nucleus in the hamster. J Comp Neurol 227:121–135.

Scott JW. 1981. Electro-physiological identification of mitral and tufted cells and distributions of their axons in olfactory system of the rat. J Neurophysiol 46:918–931.

Scott JW, McBride RL, Schneider SP. 1980. The organization of projections from the olfactory bulb to the piriform cortex and olfactory tubercle in the rat. J Comp Neurol 194:519–534.

Scott JW, Ranier EC, Pemberton JL, Orona E, Mouradian LE. 1985. Pattern of rat olfactory bulb mitral and tufted cell connections to the anterior olfactory nucleus *pars externa*. J Comp Neurol 242:415–424.

Shipley MT, Adamek GD. 1984. The connections of the mouse olfactory bulb: a study using orthograde and retrograde transport of wheat germ agglutinin conjugated to horseradish-peroxidase. Brain Res Bull 12:669–688.

Shipley MT, McLean JH, Zimmer LA, Ennis M. 1996. The olfactory system. In: Swanson LW, Björklund A, Hökfelt T, editors. Handbook of chemical neuroanatomy. Integrated systems of the CNS. Amsterdam: Elsevier. p 469–573.

Switzer RC, De Olmos J, Heimer L. 1985. Olfactory system. In: Paxinos G, editor. The rat nervous system. Sidney: Academic Press. p 1–35.

Wyss JM, Sripanidkulchai K. 1983. The indusium griseum and anterior hippocampal continuation in the rat. J Comp Neurol 219:251–272.